

# SLIDE: Saliva-Based SARS-CoV-2 Self-Testing with RT-LAMP in a Mobile Device

Zifan Tang, Jiarui Cui, Aneesh Kshirsagar, Tianyi Liu, Michele Yon, Suresh V. Kuchipudi, and Weihua Guan\*



Cite This: <https://doi.org/10.1021/acssensors.2c01023>



Read Online

ACCESS |



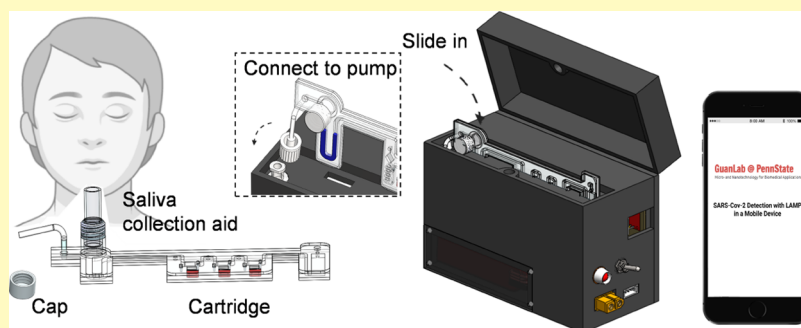
Metrics & More



Article Recommendations



Supporting Information



**ABSTRACT:** Regular, accurate, rapid, and inexpensive self-testing for severe acute respiratory syndrome coronavirus 2 (SARS-CoV-2) is urgently needed to quell pandemic propagation. The existing at-home nucleic acid testing (NAT) test has high sensitivity and specificity, but it requires users to mail the sample to the central lab, which often takes 3–5 days to obtain the results. On the other hand, rapid antigen tests for the SARS-CoV-2 antigen provide a fast sample to answer the test (15 min). However, the sensitivity of antigen tests is 30 to 40% lower than nucleic acid testing, which could miss a significant portion of infected patients. Here, we developed a fully integrated SARS-CoV-2 reverse transcription loop-mediated isothermal amplification (RT-LAMP) device using a self-collected saliva sample. This platform can automatically handle the complexity and can perform the functions, including (1) virus particles' thermal lysis preparation, (2) sample dispensing, (3) target sequence RT-LAMP amplification, (4) real-time detection, and (5) result report and communication. With a turnaround time of less than 45 min, our device achieved the limit of detection (LoD) of 5 copies/ $\mu\text{L}$  of the saliva sample, which is comparable with the LoD (6 copies/ $\mu\text{L}$ ) using FDA-approved quantitative real-time polymerase chain reaction (qRT-PCR) assays with the same heat-lysis saliva sample preparation method. With clinical samples, our platform showed a good agreement with the results from the gold-standard RT-PCR method. These results show that our platform can perform self-administrated SARS-CoV-2 nucleic acid testing by laypersons with noninvasive saliva samples. We believe that our self-testing platform will have an ongoing benefit for COVID-19 control and fighting future pandemics.

**KEYWORDS:** SARS-CoV-2, POCT, self-testing, RT-LAMP, saliva

Coronavirus disease 2019 (COVID-19) became a worldwide pandemic in early 2020,<sup>1</sup> and it was rapidly announced as a public health emergency of international concern by the World Health Organization (WHO).<sup>2,3</sup> As of March 2022, there are more than 400 million confirmed cases and 6 million deaths of severe acute respiratory syndrome coronavirus 2 (SARS-CoV-2) reported globally.<sup>3</sup> Due to the fast mutation nature of the RNA virus and so many asymptomatic cases, all countries still face an unmet need to achieve a rapid, sensitive, and reliable way to tackle the global and urgent problem. So far, a nucleic acid amplification test (NAAT), such as real-time polymerase chain reaction (RT-PCR), is the gold-standard technique due to its high sensitivity and specificity.<sup>4–7</sup> However, the laboratory-based NAAT requires highly trained personnel, dedicated facilities, and instrumentations, which typically require 3–5 days to get the result. Moreover, taking the

onsite test requires people to stay with other potential patients, increasing the exposure risk. To alleviate these bottlenecks, the COVID-19 home test has become a practical option. Two different COVID-19 home tests are available: at-home PCR test<sup>8</sup> and antigen rapid test (Ag-RDT).<sup>9,10</sup> So far, the FDA has issued EUA COVID-19 home tests developed by LabCorp, EverlyWell, Quest Diagnostics, PrivaPath Diagnostics, and Clinical Reference Laboratory. The user can self-collect the

**Received:** May 11, 2022

**Accepted:** July 14, 2022

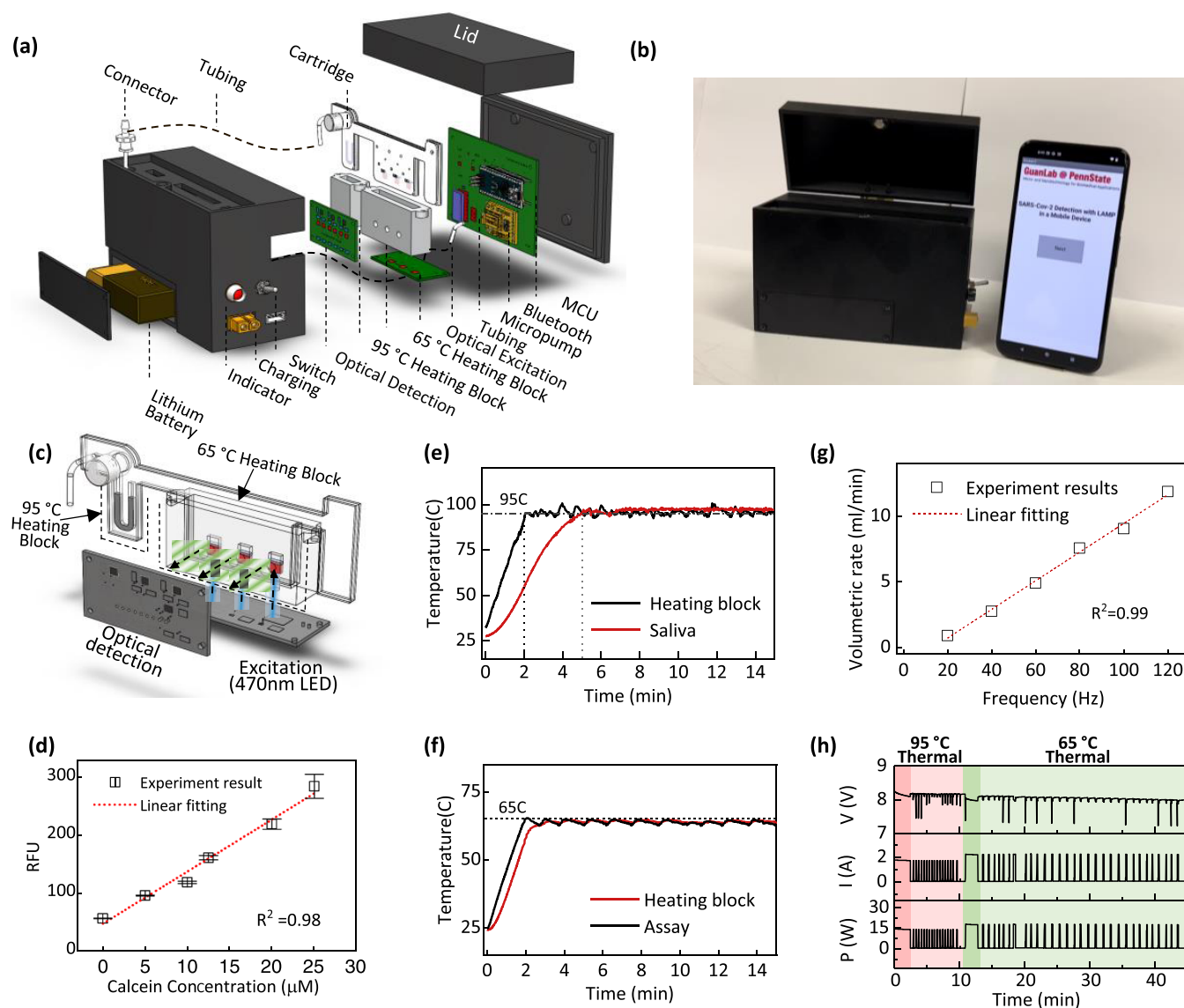


**Figure 1.** SLIDE instrument design and validation. (a) Schematic of the SLIDE device showing components in an exploded view. The platform consists of five main functional modules: optical module (light-emitting diode (LED)/optical sensor), thermal module (power resistor/thermal sensor), micro pump module, power supply module (battery), and data connectivity module (Bluetooth). Each module was controlled by a microcontroller on a customized printed circuit board (PCB). (b) Photograph of the SLIDE analyzer and the smartphone interface. (c) Schematic of the cartridge coordinated with the optical module and thermal module. (d) Characterization of the optical sensor using 40  $\mu\text{L}$  of calcein solution for 10 min of relative fluorescence unit (RFU) recording. The optical sensor showed a linear response to the concentration of calcein from 0 to 25  $\mu\text{M}$ . The temperature profile of the heating block and the liquid (saliva/assay) for (e) 95  $^{\circ}\text{C}$  virus thermal lysis and (f) 65  $^{\circ}\text{C}$  RT-LAMP reactions. (g) Characterization of the piezo pump frequency with the volumetric rate. (h) Power consumption characterization for one complete test.

sample and ship overnight to the company laboratory for SARS-CoV-2 viral RNA detection by PCR. Results are usually provided to test subjects within 3–5 days.<sup>8</sup> Even though it decreased the exposure risk, a longer time to obtain the results will increase the virus spread and delay the treatment. Ag-RDT tests are fast and cheap. It identifies active infection by detecting SARS-CoV-2 viral proteins. From sample collection to result, it takes 15–20 min using a portable device.<sup>11,12</sup> But the sensitivity of antigen tests is typically 30 to 40% lower than the nucleic acid testing.<sup>10,13,14</sup> Especially after the acute phase, when the viral load decreases, Ag-RDT might lead to high rates of false negatives, which could miss a significant portion of infected patients.<sup>9</sup>

To overcome the drawbacks of the long sample-to-result time of the conventional NAAT and the less sensitive rapid antigen

test, developing a home-used sample-in answer-out NAAT analyzer for rapid and accurate COVID-19 detection becomes extremely necessary. Molecular diagnostics typically has five essential steps: (1) lysis of cells or virus particles and DNA or RNA extraction, (2) sample partition, (3) target sequence amplification, (4) real-time detection by optical or other types of sensing mechanism,<sup>15,16</sup> and (5) data processing and result report. Integrating all of these functions in a single device is critical to achieving self-testing and speeding up the process.

Since August 2020, saliva has become an alternative sample type for SARS-CoV-2 detection.<sup>17–19</sup> This easy, noninvasive method largely increases the accessibility of self-testing.<sup>5,20–24</sup> Several studies have demonstrated that saliva has comparable performance with nasopharyngeal samples.<sup>25</sup> Moreover, this saliva sample preparation has been further simplified by the Yale

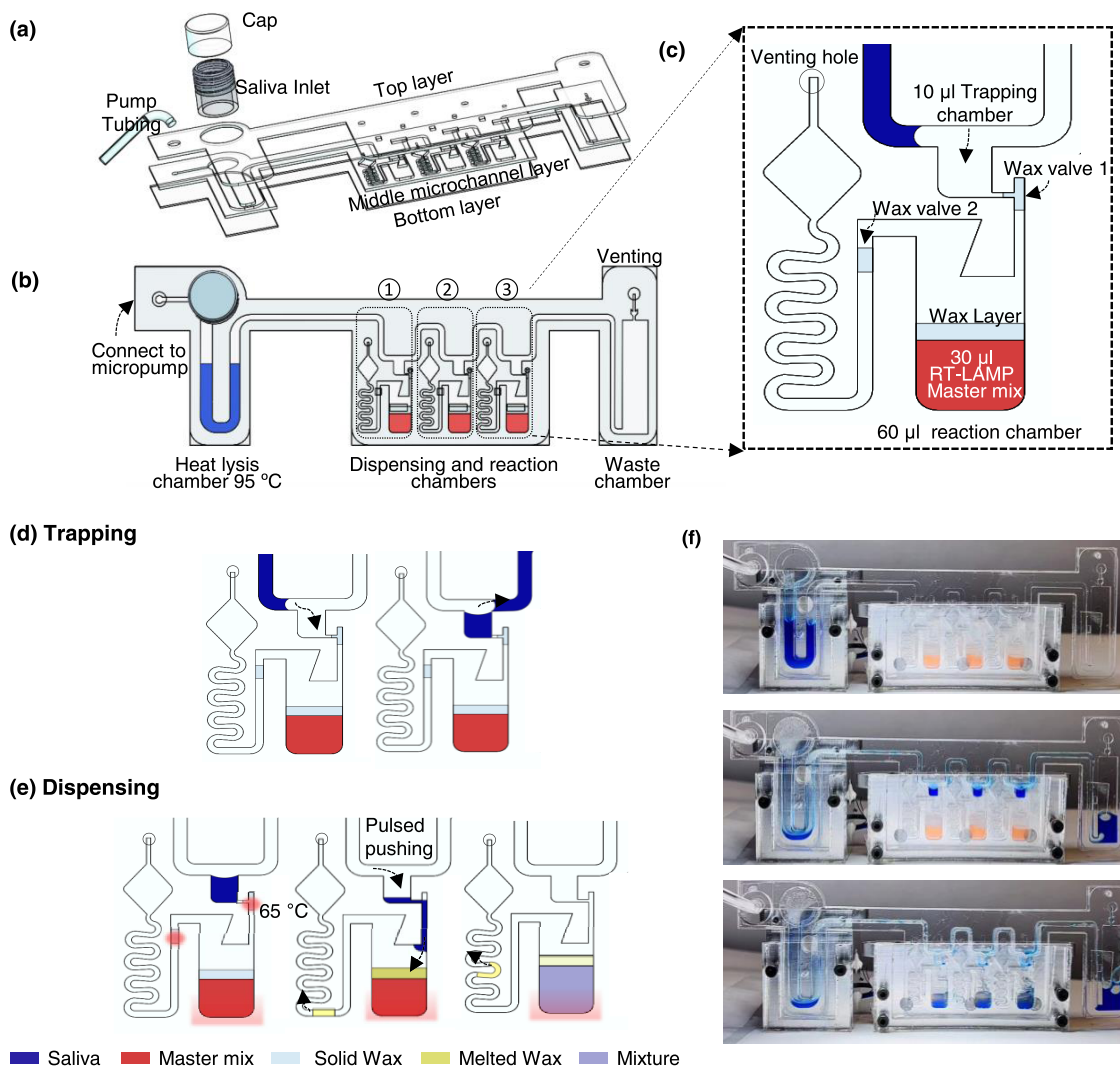


**Figure 2.** (a) Exploded view of the cartridge with three PMMA layers: top loading layer, middle microchannel layer, and bottom covering layer. (b) Assembled view of the cartridge includes a saliva collection chamber (250  $\mu\text{L}$ ), three dispensing and reaction chambers, and a waste chamber (300  $\mu\text{L}$ ). (c) One unit of the dispensing and reaction chambers comprises one trapping chamber (10  $\mu\text{L}$ ), two wax valves, and one reaction chamber (60  $\mu\text{L}$ ) with a preloaded RT-LAMP master mix and wax layer, as well as a venting hole to connect the atmosphere. Illustration of (d) trapping and (e) dispensing processes. (f) One example of sample trapping and dispensing processes (Supporting Information Video S2). The blue liquid is the saliva mixed with the blue dye, and the orange liquid is the RT-LAMP master mixed with orange dye for better visualization.

School of Public Health researcher. They found that 5 min of heat inactivation of the saliva sample without any additional reagents can achieve a low limit of detection (6 copies/ $\mu\text{L}$ ) using FDA-approved RT-PCR assays.<sup>21</sup>

Recently, isothermal amplification techniques have been widely used for the point-of-care setting, for example, reverse transcription loop-mediated isothermal amplification (RT-LAMP).<sup>5,26–42</sup> The RT-LAMP process is similar to conventional PCR tests, but the reaction can be performed without commercial thermocyclers. While maintaining specificity and sensitivity comparable to that of the PCR tests, RT-LAMP shows better tolerance for the impurities and a faster time to result. These unique features make RT-LAMP assays quicker, easier to use, and more cost-effective than RT-PCR assays, making them more suitable for point-of-care (POC) diagnostics.

In this work, we developed a fully integrated SARS-CoV-2 NAT device using a self-collected saliva sample. This saliva-based SARS-CoV-2 self-testing with RT-LAMP in a mobile device (SLIDE) platform consists of a ready-to-use reagents

cartridge, an easy-to-use smartphone interface, and an ultra-compact analyzer. It automatically handled the complexity of heat-inactivated sample preparation, sample dispensing, real-time RT-LAMP reaction and detection, and data processing. With a turnaround time of less than 45 min, we achieved a limit of detection (LoD) of 5 copies/ $\mu\text{L}$  of a saliva sample. With clinical samples, our platform showed a good agreement with the results from the gold-standard RT-PCR method. We believe that our self-testing platform will have an ongoing benefit for COVID-19 control and fighting future pandemics.

## RESULTS AND DISCUSSION

### Overall Design and Module Validation. Overall Design.

The overall design of the SLIDE analyzer is shown in Figure 1a. It consists of five seamlessly integrated modules controlled by a microcontroller unit (MCU): an optical module for excitation and detection, two thermal modules, a piezo micro pump module, a power module, and a connectivity module. Supporting Information Figure S1 illustrates the overall block

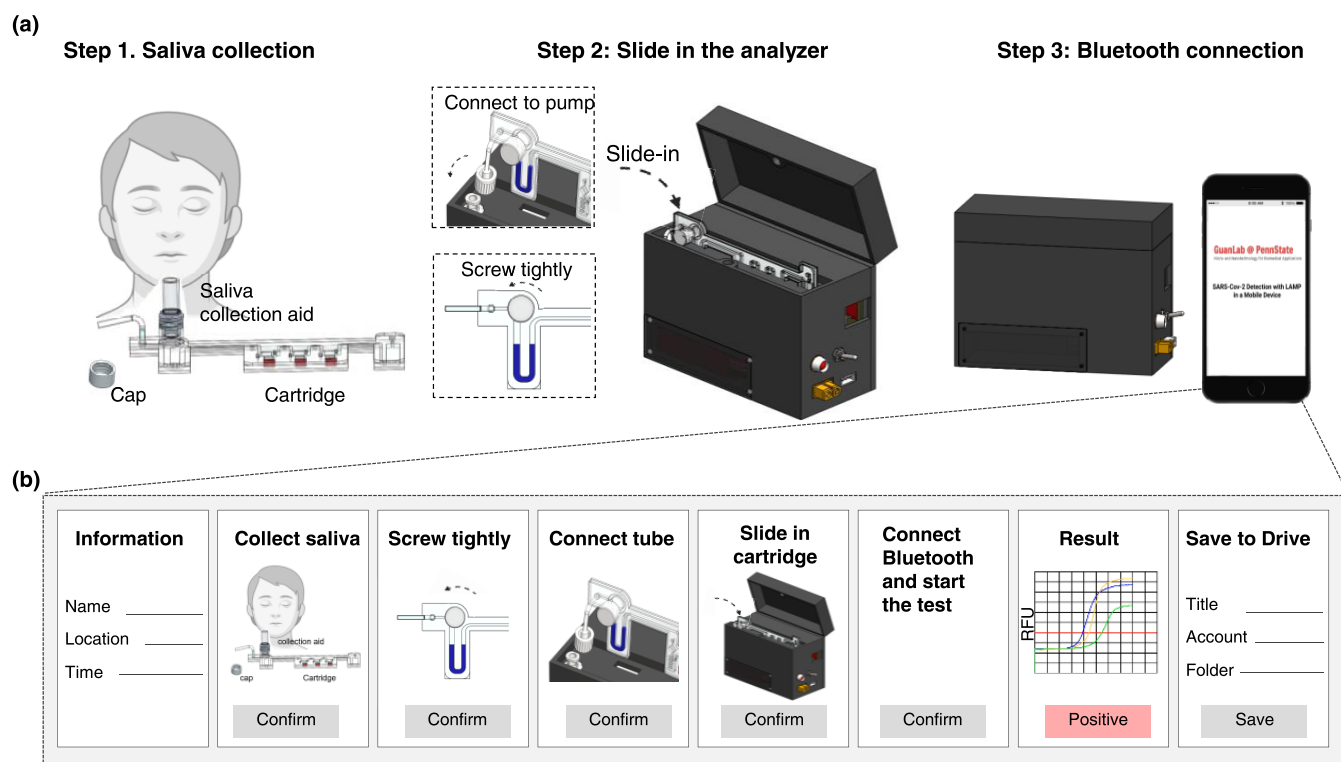


**Figure 3.** Overall SLIDE workflow. (a) Step 1: Users self-collect  $\sim 120 \mu\text{L}$  of saliva into a cartridge with the help of a saliva collection aid. Users tighten the screw cap and connect the Luer-lock to the micro pump. Step 2: The cartridge is inserted into the analyzer, and the lid is closed. Step 3: The SLIDE analyzer is connected with a smartphone through Bluetooth to initiate the test. (b) Step-by-step instruction of the App interface includes personal information collection, sample collection guidance, Bluetooth connection, test initiation, and data processing and communication.

diagram design of the device. The whole system is designed in SolidWorks and prototyped with in-house three-dimensional (3D) printing. Figure 1b shows a photograph of the assembled SLIDE analyzer and the smartphone interface.

**Optical Module.** The optical module consists of three independent excitation and detection units. Each unit has a LED excitation source ( $\lambda = 470 \text{ nm}$ ) and a complementary metal-oxide semiconductor (CMOS) color sensor for real-time fluorescence monitoring. The excitation and the detection were arranged to be perpendicular to each other to minimize the excitation interference on the fluorescence signal (Figure 1c). To characterize the quantification ability of the optical module, we tested different calcein concentrations from 0 to  $25 \mu\text{M}$  and measured the fluorescence intensity for 10 min. Figure 1d shows the mean and standard deviation of the relative fluorescence unit (RFU) as a function of the calcein concentration. A linear fit with  $R^2 = 0.98$  confirmed the quantitative capability of the optical module.

**Thermal Module.** We designed two independent thermal modules. One is for heat-inactivating the saliva and performing the thermal lysis at  $95 \text{ }^\circ\text{C}$ . The other is for controlling the temperature of the RT-LAMP reaction at  $65 \text{ }^\circ\text{C}$ . Both modules used a customized aluminum heating block with power resistors attached. The temperature was controlled through a feedback measurement of a thermistor embedded in the heating block. Since the temperature was obtained from the heating block rather than the analyte solution on the cartridge, we characterized the temperature profile difference between these two. As shown in Figure 1e, the heating block reached  $95 \text{ }^\circ\text{C}$  after 2 min of operation, while the saliva in the cartridge took 5 min. This delay is due to the nonideal thermal coupling and the different specific heat capacity between the heating block and

the cartridge. Nevertheless, saliva can be sufficiently lysed at  $95 \text{ }^\circ\text{C}$  within 10 min from sample collection. For the heating module controlling the RT-LAMP reaction, we observed that the mean and the standard deviation of the temperature in the master mix solution are 64 and  $0.38 \text{ }^\circ\text{C}$ , respectively (Figure 1f).

**Micro Pump Module.** The sample dispensing and mixing is accomplished on the cartridge using a micro piezo pump. It is connected to the microfluidic cartridge using a Tygon tube and a Luer-lock adaptor. The volumetric rate of the micro piezo pump is controlled by the frequency and the driving voltage. To characterize the micro pump, we tested the volumetric rate at different frequencies. As expected, the volumetric rate increased linearly with the operation frequency ( $R^2 = 0.99$ , Figure 1g). This relationship provides us with the capability to modulate the liquid flow rate on the cartridge through programming the operation frequency.

**Power Module.** A rechargeable 1300 mAh lithium polymer battery (14.43 Wh) was used to power our analyzer. To estimate the power consumption for each run, we used a power meter to characterize the voltage, current, and power during a complete cycle of the test. Figure 1h shows a complete time trace. As shown, heating is the most power-hungry process during the operation. Before reaching the target temperature, the heaters continuously work at a high current (1.7 A for  $95 \text{ }^\circ\text{C}$  and 2.2 A for  $65 \text{ }^\circ\text{C}$ ). After reaching the target temperature, the heater starts to change states between on and off to maintain the temperature. The total energy consumed is 3.02 Wh in each 45 min test, meaning we can perform at least four tests before recharging.

**Connectivity Module.** A smartphone app was developed to assist the user in conducting the test. The flow chart of the app process is shown in Supporting Information Figure S2. The

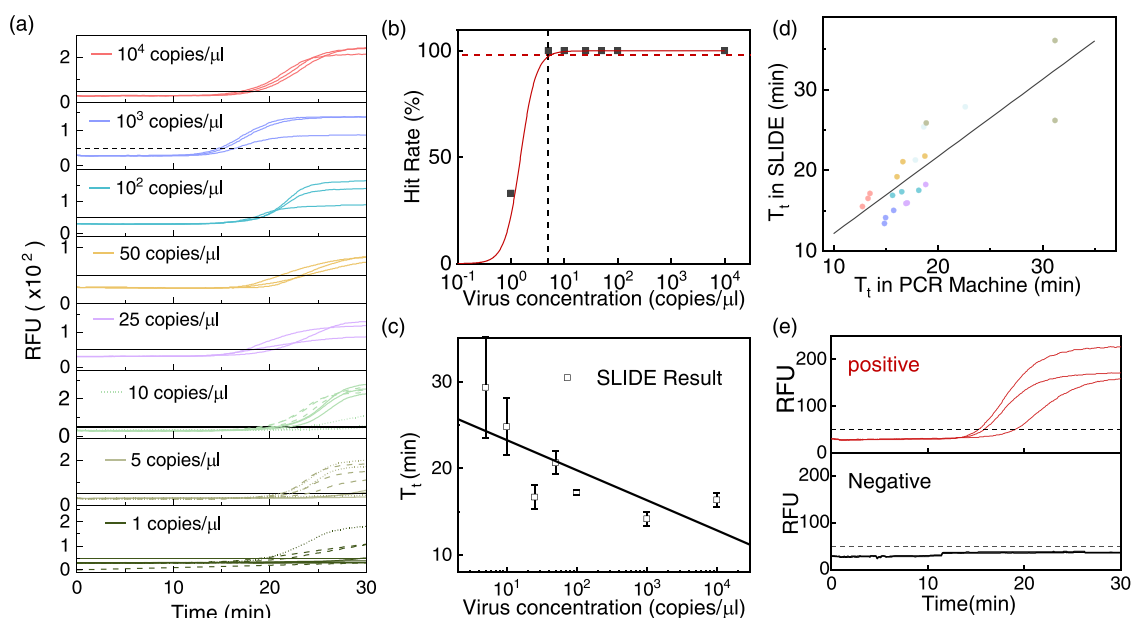


**Figure 4.** SLIDE device performance evaluation. (a) Real-time RT-LAMP results with different concentrations of the spiked saliva samples (1 copy/ $\mu\text{L}$  to  $10^4$  copies/ $\mu\text{L}$ ) using a SLIDE analyzer. The threshold to classify an amplification curve as positive or negative was 50 RFU based on the NTC sample (Supporting Information Figure S5). (b) Extracted hit rate at various virus particle concentrations to establish LoD. (c) Inversely proportional relationship between the threshold time ( $T_t$ ) and virus particle concentration was obtained from the SLIDE analyzer. (d) Pearson correlation analysis of the  $T_t$  between the manual operation with a PCR machine and automatic method using the SLIDE analyzer. (e) Two clinical samples, one known positive (top) and one known negative (bottom), were tested by the SLIDE device. The initial diagnosis was performed by the RT-PCR assay as the reference.

SLIDE analyzer and the smartphone communicated through the Bluetooth LE protocol. The App could provide test instructions, acquire data, and make positive and negative calls to interpret the test results. The App could also save the test results into a spreadsheet, save them on the local smartphone, or upload them to cloud-based storage (Google Drive). Supporting Information Figure S3 shows the representative screenshots of the developed App.

**Automated Saliva Processing on the Cartridge.** To facilitate the raw saliva processing, we developed a disposable cartridge with the SLIDE analyzer. The cartridge was fabricated in poly(methyl methacrylate) (PMMA). It consists of three laminated layers: top layer, middle microchannel layer, and bottom layer (Figure 2a). The overall layout of the assembled cartridge is shown in Figure 2b. It includes a heat-lysis chamber (250  $\mu\text{L}$ ), three independent dispensing (10  $\mu\text{L}$ ) and reaction chambers (60  $\mu\text{L}$ ), and a waste chamber (300  $\mu\text{L}$ ). First, the collected raw saliva sample was heat-inactivated and lysed at 95  $^\circ\text{C}$  for 5 min. The resulting lysates were transferred to the dispensing and reaction chambers through the microchannel. The excessive analyte sample was stored in the waste chamber with a venting hole to the atmospheric pressure.

Figure 2c illustrates the detailed design of a single unit of dispensing and reaction chambers. Since the laser-processed PMMA side walls are hydrophilic,<sup>43</sup> a side pocket structure can easily trap 10  $\mu\text{L}$  of the samples without bubbles. We found that the 5.3 mL/min flow rate could help ensure the reliable trapping process. During the trapping process, the paraffin wax valve 1 was in the solid phase such that the trapping volume was fixed (Figure 2d). The average trapping volume is  $10.25 \pm 0.27 \mu\text{L}$ . The difference between the three chambers was less than 2.5% (Supporting Information Figure S4).

After excessive samples were pushed into the waste chamber and each unit metered 10  $\mu\text{L}$  of the heat-processed saliva, we

increased the temperature to 65  $^\circ\text{C}$  to open the paraffin wax valves. When the wax valves 1 and 2 change from the solid to the liquid phase, the trapped saliva sample will start flowing into the reaction chamber by capillary force. To facilitate transferring all samples into the reaction chamber and thorough mixing with the RT-LAMP master mix, we applied 30 consecutive micro pump pressure pulses. Each pulse is programmed to be 100 ms in duration (Figure 2e). The paraffin wax valve 2 serves as a hydraulic resistor, which helps to balance the hydraulic resistance among three units. To avoid liquid overflowing, we intentionally designed a long S-shaped releasing channel with a venting hole at the end. In addition, a thin layer of wax on top of the RT-LAMP mix protects the master mix from evaporation. It also avoids external contamination by providing a barrier against amplicons from escaping. Figure 2f and Supporting Information Video S1 show a representative example of automated saliva processing on the cartridge.

**Saliva Test Workflow.** The overall SLIDE workflow from the saliva sample to the molecular results is shown in Figure 3a. Four components are needed for a test: a disposable cartridge, a saliva collection aid (SCA), a portable analyzer, and an Android smartphone. With the help of the instructions on an interactive smartphone app (Figure 3b), one would self-collect saliva samples into a cartridge with the help of an SCA. While collecting the whole saliva through spitting or drooling is feasible, the saliva collection aid could increase participant compliance and avoid sample foaming.<sup>21</sup> After sufficient saliva ( $\sim 120 \mu\text{L}$ ) was collected into the cartridge, the user should seal the cartridge with a screw cap. The sealed cartridge can then be connected to the piezo pump through a Luer-lock interface and be inserted into the analyzer. One then would need to turn on the analyzer for the smartphone to recognize and communicate through the Bluetooth connection. This process takes less than 2 min hands-on time and is the only manual testing step.

Once the SLIDE analyzer receives the “start testing” command from the smartphone app, the analyzer will automatically perform the required tasks on the cartridge. It includes saliva thermal lysis, sample metering and dispensing, RT-LAMP reaction and real-time detection, and data analysis and storage. Specifically, the analyzer begins the test by thermal lysis of the saliva sample at 95 °C for 5 min. This step inactivates RNases and releases the virus from the saliva sample.<sup>21</sup> The resulting lysates were automatically transferred and dispensed into the reaction chamber with a preloaded RT-LAMP master. The whole sample preparation takes about 13 min. After dispensing the sample, the real-time RT-LAMP reaction starts at a constant temperature of ~64 °C.<sup>41</sup> The acquired fluorescence data are transmitted to the smartphone app every 5 s. The threshold to distinguish the positive from the negative was set at 50 RFU based on the no template control (NTC) samples tested (Supporting Information Figure S5). We classify a sample as positive only when two out of three reactions have a higher RFU than the threshold value in 30 min. The test results could be saved on the local device and uploaded to a cloud. The whole process is fully automated (Supporting Information Figure S6) and takes about less than 45 min (~2 min hands-on time for sample collection, ~13 min for sample preparation and dispensing, and ~15–30 min for the RT-LAMP reaction, and data processing and result report) from the saliva collection to the result, with very minimal user intervention (Supporting Information Video S2).

#### Performance Evaluation with the Mock Saliva Sample.

After validating all of the subsystems and system integration, we went out to test the performance of the SLIDE. Here, we used our previously validated SARS-CoV-2 RT-LAMP primer set<sup>41</sup> (Supporting Information Table S1) against the highly conserved N region with a modified fluorescent concentration of SYTO9 (Supporting Information Table S2). We formed mock SARS-CoV-2 positive samples by spiking the healthy saliva with different concentrations of heat-inactivated SARS-CoV-2 virus particles. The final viral concentration of the mock sample ranges from 1 to 10<sup>4</sup> copies/ $\mu$ L. Figure 4a shows the real-time result. Note that each sample is aliquoted to three separate reactions on a single cartridge (Figure 2b). The sample is classified as positive in each test only if more than two out of three reactions have an RFU of more than a threshold. As shown, samples with a concentration above 5 copies/ $\mu$ L were successfully classified as positive, while one out of three samples at 1 copy/ $\mu$ L were classified as positive.

To estimate the LoD of the test, we examined the hit rates at different virus concentrations.<sup>44</sup> The hit rate is the positive test over all of the tests under the same concentration. As shown in Figure 4b, the hit rate started to roll off from 100 to 33% when the concentration decreased from 5 copies/ $\mu$ L to 1 copy/ $\mu$ L. We fitted the experimental hit rate data with a logistic curve. The LoD is determined to be about 5 copies/ $\mu$ L at the 98% confidence level. This LoD is comparable with the LoD (6 copies/ $\mu$ L) using FDA-approved quantitative RT-PCR (qRT-PCR) assays with the same heat-lysis saliva sample preparation method.<sup>21</sup> Figure 4c shows the threshold time in the SLIDE analyzer with different virus concentrations. The threshold time and the standard deviation among the times to positive generally increase as the virus particle concentration decreases, although the linearity is not as good as a RT-PCR test. The less ideal linearity is expected as the RT-LAMP assay is not a quantitative assay.

To further evaluate our device, the same spike samples were tested using the benchtop PCR machine. We manually performed the sample thermal lysis in the heating block for 5 min at 95 °C and then transferred 10  $\mu$ L of the processed sample using a pipette to the PCR tube with a preloaded RT-LAMP master mix. After mixing the reagents thoroughly, the reactions were performed using a benchtop PCR machine (Supporting Information Figure S7). Figure 4d shows a Pearson correlation of the threshold time between the SLIDE analyzer and the PCR instrument. A coefficient ( $R = 0.835$ ) indicates a good agreement between the automated SLIDE device and manual methods.

**Clinical Saliva Sample Test.** To best evaluate the performance of SLIDE, clinical samples were tested. Here, two archived clinical samples (one known positive and one known negative) were obtained through an approved institutional review board (IRB) of the Pennsylvania State University. All of the samples were coded to remove information associated with patient identifiers. The RT-PCR assay performed the initial diagnosis as the reference method to benchmark our SLIDE. The experiment follows the protocols shown in Figure 3 and Supporting Information Video S2. The resulting raw amplification curves are shown in Figure 4e. In 30 min of the amplification process, all three reactions in the positive test showed sharp RFU increases and stabilized at the RFU value at least three times above the threshold. All reactions in the negative clinical sample showed no noticeable RFU changes. The positive and negative samples determined by the SLIDE analyzer agree with that of the gold-standard RT-PCR method. Evaluating more clinical samples would be needed to demonstrate the device robustness and reproducibility. A scaled-up test with more clinical samples is currently under another IRB approval. We will evaluate and report the diagnostic sensitivity and specificity of the SLIDE device when these data are acquired in the future.

## CONCLUSIONS

We demonstrated a fully integrated device for rapid (<45 min) self-testing of the SARS-CoV-2 virus from saliva samples. This fully portable device can detect the virus rapidly without needing an RNA extraction kit and pipetting steps. All other complexities are handled automatically by the SLIDE analyzer, including sample processing and dispensing, real-time RT-LAMP reaction and detection, and data processing and communication. Our automatic system shows an excellent agreement with the manual process using a benchtop PCR instrument. The limit of detection against the SARS-CoV-2 virus particle spiked in the saliva sample is 5 copies/ $\mu$ L. This LoD is comparable with the LoD (6 copies/ $\mu$ L) using FDA-approved qRT-PCR assays with the same heat-lysis saliva sample preparation method.<sup>21</sup> A pilot clinical saliva sample test with the SLIDE showed a good agreement with the gold-standard RT-PCR method. These results show that it is feasible to perform self-administrated SARS-CoV-2 nucleic acid testing by laypersons with non-invasive saliva samples. To that end, we will need to further address the outstanding issues of reagent lyophilization on the cartridge and scaled-up clinical validation in future studies.

## MATERIALS AND METHODS

**SARS-CoV-2 Samples.** Heat-inactivated SARS-CoV-2 (ATCC VR-1986HK) virus particles were purchased from ATCC. The negative saliva samples were collected from healthy volunteers. The mock samples were prepared by spiking the heat-inactivated SARS-CoV-2 virus particles into the healthy saliva sample. The reidentified clinical

saliva samples were approved by the institutional review board (IRB). These clinical saliva samples were initially tested with the FDA EUA-authorized OPTI RT-PCR COVID-19 direct assay (OPTI Medical Systems, GA). The collected saliva samples were frozen at  $-80\text{ }^{\circ}\text{C}$  before use. All clinical experiments were performed in the Animal Diagnostic Laboratory (BSL 3) at Penn State (University Park) by a protocol approved by the Institutional Biosafety Committee.

**RT-LAMP Reaction Mix.** The total volume ( $40\text{ }\mu\text{L}$ ) of the RT-LAMP assays contains a  $30\text{ }\mu\text{L}$  of master mix and  $10\text{ }\mu\text{L}$  of the saliva sample. The master mix includes isothermal buffer, PCR-grade  $\text{H}_2\text{O}$ ,  $\text{MgSO}_4$  ( $7\text{ mM}$ ), Styo-9 green ( $10\text{ }\mu\text{M}$ ), deoxyribonucleotide triphosphates (dNTPs,  $1.4\text{ mM}$ ), Bst 2.0 DNA polymerase ( $0.4\text{ U}/\mu\text{L}$ ), WarmStart reverse transcriptase ( $0.3\text{ U}/\mu\text{L}$ ), and primer sets ( $0.2\text{ mM}$  F3 and B3c,  $1.6\text{ mM}$  FIP and BIP,  $0.8\text{ mM}$  LF and LB, see Supporting Information Table S1 for primer design). Supporting Information Table S2 summarizes the RT-LAMP recipe.

**Instrumentation.** Figure 1a shows a photo of a SLIDE analyzer. The SLIDE analyzer comprises 3D printed structural parts, a CNC machined aluminum heating block, a micro pump, and electronics such as an Arduino Nano (MCU), excitation LEDs, and color sensors for fluorescence detection and Bluetooth. The 3D housing was designed in Solidworks software and printed using a MakerBot MethodX 3D printer (Brooklyn, NY) with MakerBot ABS (acrylonitrile butadiene styrene). The aluminum heating blocks were designed in Solidworks software and fabricated using a CNC machine. Two one-ohm power resistors are mounted (in series) on the aluminum heating using a thermally conductive adhesive paste for the  $95\text{ }^{\circ}\text{C}$  heating block and  $65\text{ }^{\circ}\text{C}$  heating block, respectively. Negative thermal feedback control was performed using an N-channel power MOSFET (63J7707, Digi-Key) and an MC65F103A 10 k-ohm thermistor (Amphenol Thermometrics, St. Marys, PA) to maintain the desired temperature. PCBs were designed in AutoDesk Eagle CAD software and fabricated by O.S.H. Park L.L.C. (Lake Oswego, OR). The optical module PCB consists of three blue excitation LEDs (FD-5TB-1) purchased from Adafruit Industries (New York, NY) and three-color sensors (TCS 34725) purchased from Digi-Key. The piezo pump and the driver were purchased from Bartels (Mikrotechnik, Germany). The Bluetooth (Adafruit Bluefruit LE SPI Friend) module was purchased from Adafruit Industries (New York, NY). The whole system was powered by a 1300 mAh Lithium polymer battery (ZIPPIY). All materials of the analyzer can be found in Supporting Information Table S3.

**App Development.** Four steps are involved in this Android App development. First, the App interface guides users in providing their personal information. Only the name is required from users. The global positioning system (GPS) can automatically obtain the time and location information. Second, we set up Bluetooth communication. App interface scans and connects the Bluetooth LE around the analyzer. The communication protocol can be built using the service UUID and characteristic UUID of the Bluetooth LE, enabling the data communication function between these two devices. Once the user clicks the confirm button on the screen, the App will send a single bit to the analyzer to initiate the test. The third part is the real-time data transfer and plotting. We added two check bits at the beginning and the end of the string to ensure accuracy. After confirming the check bit of the received string from the analyzer, the string value will be split into three channels and plotted with different colors. Meanwhile, the split data in each channel is compared with the threshold value (RFU 50) to make the decision. If more than or equal to two channels have three successive data greater than the threshold, the test result will be identified as a positive. Otherwise, the App will continue to receive the string value from the analyzer. If no positive result has been determined after 30 min of the amplification, the test result will be negative. The App will combine personal information, color sensor data in each channel, and test results into a spreadsheet. This file can be saved on the local device and uploaded to a Google drive. The flow chart of this App development process is shown in Supporting Information Figure S2. Selected screenshots of the App are presented in Supporting Information Figure S3.

**Microfluidic Reagent Cartridge.** The microfluidic cartridge was designed by AutoCAD and patterned using a  $\text{CO}_2$  laser cutting machine

(Universal Laser Systems, Scottsdale, AZ). All layers were aligned and laminated with an adhesive solvent (Weld-On). The assembled cartridge comprises a sample collection chamber ( $250\text{ }\mu\text{L}$ ), three trapping chambers ( $10\text{ }\mu\text{L}$  each), three reaction chambers ( $60\text{ }\mu\text{L}$  each), three wax valves 1 ( $5\text{ }\mu\text{L}$  each), three wax valves 2 ( $5\text{ }\mu\text{L}$  each), and waste chamber ( $300\text{ }\mu\text{L}$ ). The sample collection tube was mounted using the epoxy adhesive (3M, Saint Paul, MN). All of the assay and wax valves were loaded onto the cartridge through the extruded inlet and sealed by the PCR plate seals (Bio-Rad, Hercules, CA). The saliva collection aid was purchased from Salimetrics, LLC.

**Data Processing.** To find the proper threshold, all of the collected raw data were subtracted from the background signal acquired from the average of the first 10 data points and leveled at RFU 30. The threshold to classify an amplification curve as positive or negative was 50 RFU based on the negative sample (Supporting Information Figure S5).

## ■ ASSOCIATED CONTENT

### Supporting Information

The Supporting Information is available free of charge at <https://pubs.acs.org/doi/10.1021/acssensors.2c01023>.

Analyzer system diagram; flow chart of the android App development; mobile phone user interface; trapping volume characterization; representative measurement from negative control samples; flow chart of the automatic workflow from the sample to answer; real-time results using a PCR machine; detailed descriptions of the RT-LAMP primer set for the N region; recipe for RT-LAMP master mix; and bill of the material for the SLIDE analyzer (PDF)

Workflow of the saliva-based SARS-CoV-2 self-testing with RT-LAMP (MP4)

Representative cases of the automatic sample dispensing on the cartridge (MP4)

## ■ AUTHOR INFORMATION

### Corresponding Author

Weihua Guan – Department of Electrical Engineering, Pennsylvania State University, University Park, Pennsylvania 16802, United States; Department of Biomedical Engineering, Pennsylvania State University, University Park, Pennsylvania 16802, United States; [orcid.org/0000-0002-8435-9672](https://orcid.org/0000-0002-8435-9672); Email: [wzg111@psu.edu](mailto:wzg111@psu.edu)

### Authors

Zifan Tang – Department of Electrical Engineering, Pennsylvania State University, University Park, Pennsylvania 16802, United States

Jiarui Cui – Department of Electrical Engineering, Pennsylvania State University, University Park, Pennsylvania 16802, United States

Aneesh Kshirsagar – Department of Electrical Engineering, Pennsylvania State University, University Park, Pennsylvania 16802, United States; [orcid.org/0000-0003-2288-5439](https://orcid.org/0000-0003-2288-5439)

Tianyi Liu – Department of Electrical Engineering, Pennsylvania State University, University Park, Pennsylvania 16802, United States

Michele Yon – Animal Diagnostic Laboratory, Pennsylvania State University, University Park, Pennsylvania 16802, United States

Suresh V. Kuchipudi – Animal Diagnostic Laboratory and Center for Infectious Disease Dynamic, Pennsylvania State University, University Park, Pennsylvania 16802, United States

Complete contact information is available at:

<https://pubs.acs.org/10.1021/acssensors.2c01023>

### Author Contributions

W.G. conceived the concept and supervised the study. Z.T., A.K., and T.L. developed the instrument and integration. Z.T. and J.C. developed the mobile App. Z.T. developed and validated the RT-LAMP, cartridge design, and the device. Z.T., S.V.K., and M.Y. performed the clinical sample study. Z.T. and W.G. co-wrote the manuscript, with discussion from all authors.

### Notes

The authors declare the following competing financial interest(s): A provisional patent related to the technology described herein is filed.

A provisional patent related to the technology described herein is filed.

### ACKNOWLEDGMENTS

This work was supported by the National Institutes of Health (R61AI147419), National Science Foundation (1902503, 1912410, 2045169), and Coronavirus Research Seed Fund. Any opinions, findings, and conclusions or recommendations expressed in this work are those of the authors and do not necessarily reflect the views of the National Science Foundation and National Institutes of Health.

### REFERENCES

- (1) Harapan, H.; Itoh, N.; Yufika, A.; Winardi, W.; Keam, S.; Te, H.; Megawati, D.; Hayati, Z.; Wagner, A. L.; Mudatsir, M. Coronavirus disease 2019 (COVID-19): A literature review. *J. Infect. Public Health* **2020**, *13*, 667–673.
- (2) Zhu, N.; Zhang, D.; Wang, W.; Li, X.; Yang, B.; Song, J.; Zhao, X.; Huang, B.; Shi, W.; Lu, R.; et al. A novel coronavirus from patients with pneumonia in China, 2019. *N. Engl. J. Med.* **2020**, *382*, 727–733.
- (3) Kwok, H.; Briggs, K.; Tabard-Cossa, V. Nanopore Fabrication by Controlled Dielectric Breakdown. *PLoS one* **2014**, *9*, No. e92880.
- (4) Chan, J. F.-W.; Yip, C. C.-Y.; To, K. K.-W.; Tang, T. H.-C.; Wong, S. C.-Y.; Leung, K.-H.; Fung, A. Y.-F.; Ng, A. C.-K.; Zou, Z.; Tsoi, H.-W.; et al. Improved molecular diagnosis of COVID-19 by the novel, highly sensitive and specific COVID-19-RdRp/Hel real-time reverse transcription-PCR assay validated in vitro and with clinical specimens. *J. Clin. Microbiol.* **2020**, *58*, No. e00310-20.
- (5) Nagura-Ikeda, M.; Imai, K.; Tabata, S.; Miyoshi, K.; Murahara, N.; Mizuno, T.; Horiuchi, M.; Kato, K.; Imoto, Y.; Iwata, M.; et al. Clinical evaluation of self-collected saliva by quantitative reverse transcription-PCR (RT-qPCR), direct RT-qPCR, reverse transcription–loop-mediated isothermal amplification, and a rapid antigen test to diagnose COVID-19. *J. Clin. Microbiol.* **2020**, *58*, No. e01438-20.
- (6) Tahamtan, A.; Ardebili, A. Real-time RT-PCR in COVID-19 detection: issues affecting the results. *Expert Rev. Mol. Diagn.* **2020**, *20*, 453–454.
- (7) Vogels, C. B. F.; Brito, A. F.; Wyllie, A. L.; Fauver, J. R.; Ott, I. M.; Kalinich, C. C.; Petrone, M. E.; Casanovas-Massana, A.; Muenker, M. C.; Moore, A. J.; et al. Analytical sensitivity and efficiency comparisons of SARS-CoV-2 RT–qPCR primer–probe sets. *Nat. Microbiol.* **2020**, *5*, 1299–1305.
- (8) Liao, W. T.; Hsu, M. Y.; Shen, C. F.; Hung, K. F.; Cheng, C. M. Home Sample Self-Collection for COVID-19 Patients. *Adv. Biosyst.* **2020**, *4*, No. 2000150.
- (9) Mak, G. C.; Cheng, P. K.; Lau, S. S.; Wong, K. K.; Lau, C.; Lam, E. T.; Chan, R. C.; Tsang, D. N. Evaluation of rapid antigen test for detection of SARS-CoV-2 virus. *J. Clin. Virol.* **2020**, *129*, No. 104500.
- (10) Dinnes, J.; Deeks, J. J.; Adriano, A.; Berhane, S.; Davenport, C.; Ditttrich, S.; Emperador, D.; Takwoingi, Y.; Cunningham, J.; Beese, S.; Dretzke, J.; Ferrante di Ruffano, L.; Harris, I. M.; Price, M. J.; Taylor-Phillips, S.; Hooft, L.; Leeflang, M. M. G.; Spijker, R.; Van den Bruel, A. Rapid, point-of-care antigen and molecular-based tests for diagnosis of

SARS-CoV-2 infection *Cochrane Database Systematic Reviews* 2020 Issue 8. Art. No. CD013705. DOI: 10.1002/14651858.CD013705.

- (11) Albert, E.; Torres, I.; Bueno, F.; Huntley, D.; Molla, E.; Fernández-Fuentes, M. Á.; Martínez, M.; Poujois, S.; Forqué, L.; Valdivia, A.; et al. Field evaluation of a rapid antigen test (Panbio COVID-19 Ag Rapid Test Device) for COVID-19 diagnosis in primary healthcare centres. *Clin. Microbiol. Infect.* **2021**, *27*, 472.e7–472.e10.

- (12) Torres, I.; Poujois, S.; Albert, E.; Colomina, J.; Navarro, D. Evaluation of a rapid antigen test (Panbio COVID-19 Ag rapid test device) for SARS-CoV-2 detection in asymptomatic close contacts of COVID-19 patients. *Clin. Microbiol. Infect.* **2021**, *27*, 636.e1–636.e4.

- (13) Scohy, A.; Anantharajah, A.; Bodéus, M.; Kabamba-Mukadi, B.; Verroken, A.; Rodriguez-Villalobos, H. Low performance of rapid antigen detection test as frontline testing for COVID-19 diagnosis. *J. Clin. Virol.* **2020**, *129*, No. 104455.

- (14) Brümmer, L. E.; Katzenschlager, S.; Gaeddert, M.; Erdmann, C.; Schmitz, S.; Bota, M.; Grilli, M.; Larmann, J.; Weigand, M. A.; Pollock, N. R.; et al. Accuracy of novel antigen rapid diagnostics for SARS-CoV-2: A living systematic review and meta-analysis. *PLoS Med.* **2021**, *18*, No. e1003735.

- (15) Taleghani, N.; Taghipour, F. Diagnosis of COVID-19 for controlling the pandemic: A review of the state-of-the-art. *Biosens. Bioelectron.* **2021**, *174*, No. 112830.

- (16) Nguyen, H. V.; Nguyen, V. D.; Nguyen, H. Q.; Chau, T. H. T.; Lee, E. Y.; Seo, T. S. Nucleic acid diagnostics on the total integrated lab-on-a-disc for point-of-care testing. *Biosens. Bioelectron.* **2019**, *141*, No. 111466.

- (17) Kojima, N.; Turner, F.; Slepnev, V.; Bacelar, A.; Deming, L.; Kodeboyina, S.; Klausner, J. Self-Collected Oral Fluid and Nasal Swabs Demonstrate Comparable Sensitivity to Clinician Collected Nasopharyngeal Swabs for Coronavirus Disease 2019 Detection. *Clin. Infect. Dis.* **2021**, *73*, e3106–e3109.

- (18) Williams, E.; Bond, K.; Zhang, B.; Putland, M.; Williamson, D. A. Saliva as a Noninvasive Specimen for Detection of SARS-CoV-2. *J. Clin. Microbiol.* **2020**, *58*, No. e00776-20.

- (19) Pasomsub, E.; Watcharananan, S. P.; Boonyawat, K.; Janchompoo, P.; Wongtabtim, G.; Suksuwan, W.; Sungkanuparph, S.; Phuphuakrat, A. Saliva sample as a non-invasive specimen for the diagnosis of coronavirus disease 2019: a cross-sectional study. *Clin. Microbiol. Infect.* **2021**, *27*, 285.e1–285.e4.

- (20) Wyllie, A. L.; Fournier, J.; Casanovas-Massana, A.; Campbell, M.; Tokuyama, M.; Vijayakumar, P.; Warren, J. L.; Geng, B.; Muenker, M. C.; Moore, A. J.; et al. Saliva or nasopharyngeal swab specimens for detection of SARS-CoV-2. *N. Engl. J. Med.* **2020**, *383*, 1283–1286.

- (21) Vogels, C. B.; Watkins, A. E.; Harden, C. A.; Brackney, D. E.; Shafer, J.; Wang, J.; Caraballo, C.; Kalinich, C. C.; Ott, I. M.; Fauver, J. R.; et al. SalivaDirect: A simplified and flexible platform to enhance SARS-CoV-2 testing capacity. *Med* **2021**, *2*, 263–280.

- (22) Ning, B.; Yu, T.; Zhang, S.; Huang, Z.; Tian, D.; Lin, Z.; Niu, A.; Golden, N.; Hensley, K.; Threeton, B.; et al. A smartphone-read ultrasensitive and quantitative saliva test for COVID-19. *Sci. Adv.* **2021**, *7*, No. eabe3703.

- (23) Lalli, M. A.; Langmade, J. S.; Chen, X.; Fronick, C. C.; Sawyer, C. S.; Burcea, L. C.; Wilkinson, M. N.; Fulton, R. S.; Heinz, M.; Buchser, W. J.; et al. Rapid and extraction-free detection of SARS-CoV-2 from saliva by colorimetric reverse-transcription loop-mediated isothermal amplification. *Clin. Chem.* **2021**, *67*, 415–424.

- (24) Azzi, L.; Carcano, G.; Gianfagna, F.; Grossi, P.; Dalla Gasperina, D.; Genoni, A.; Fasano, M.; Sessa, F.; Tettamanti, L.; Carinci, F.; et al. Saliva is a reliable tool to detect SARS-CoV-2. *J. Infect.* **2020**, *81*, e45–e50.

- (25) Butler-Laporte, G.; Lawandi, A.; Schiller, I.; Yao, M.; Dendukuri, N.; McDonald, E. G.; Lee, T. C. Comparison of saliva and nasopharyngeal swab nucleic acid amplification testing for detection of SARS-CoV-2: a systematic review and meta-analysis. *JAMA Intern. Med.* **2021**, *181*, 353–360.

- (26) Notomi, T.; Okayama, H.; Masubuchi, H.; Yonekawa, T.; Watanabe, K.; Amino, N.; Hase, T. Loop-mediated isothermal amplification of DNA. *Nucleic Acids Res.* **2000**, *28*, No. e63.



- (27) Parida, M.; Sannarangaiah, S.; Dash, P. K.; Rao, P.; Morita, K. Loop mediated isothermal amplification (LAMP): a new generation of innovative gene amplification technique; perspectives in clinical diagnosis of infectious diseases. *Rev. Med. Virol.* **2008**, *18*, 407–421.
- (28) Subramanian, S.; Gomez, R. D. An empirical approach for quantifying loop-mediated isothermal amplification (LAMP) using *Escherichia coli* as a model system. *PLoS One* **2014**, *9*, No. e100596.
- (29) Roy, S.; Wei, S. X.; Ying, J. L. Z.; Safavieh, M.; Ahmed, M. U. A novel, sensitive and label-free loop-mediated isothermal amplification detection method for nucleic acids using luminophore dyes. *Biosens. Bioelectron.* **2016**, *86*, 346–352.
- (30) Tang, Z.; Choi, G.; Nouri, R.; Guan, W. Loop-Mediated Isothermal Amplification-Coupled Glass Nanopore Counting Toward Sensitive and Specific Nucleic Acid Testing. *Nano Lett.* **2019**, *19*, 7927–7934.
- (31) Baek, Y. H.; Um, J.; Antigua, K. J. C.; Park, J.-H.; Kim, Y.; Oh, S.; Kim, Y.-i.; Choi, W.-S.; Kim, S. G.; Jeong, J. H.; et al. Development of a reverse transcription-loop-mediated isothermal amplification as a rapid early-detection method for novel SARS-CoV-2. *Emerging Microbes Infect.* **2020**, *9*, 998–1007.
- (32) Ganguli, A.; Mostafa, A.; Berger, J.; Aydin, M. Y.; Sun, F.; de Ramirez, S. A. S.; Valera, E.; Cunningham, B. T.; King, W. P.; Bashir, R. Rapid isothermal amplification and portable detection system for SARS-CoV-2. *Proc. Natl. Acad. Sci. U.S.A.* **2020**, *117*, 22727–22735.
- (33) Jiang, M.; Pan, W.; Arasthfer, A.; Fang, W.; Ling, L.; Fang, H.; Daneshnia, F.; Yu, J.; Liao, W.; Pei, H.; et al. Development and validation of a rapid, single-step reverse transcriptase loop-mediated isothermal amplification (RT-LAMP) system potentially to be used for reliable and high-throughput screening of COVID-19. *Front. Cell. Infect. Microbiol.* **2020**, *10*, No. 331.
- (34) Kitagawa, Y.; Orihara, Y.; Kawamura, R.; Imai, K.; Sakai, J.; Tarumoto, N.; Matsuoka, M.; Takeuchi, S.; Maesaki, S.; Maeda, T. Evaluation of rapid diagnosis of novel coronavirus disease (COVID-19) using loop-mediated isothermal amplification. *J. Clin. Virol.* **2020**, *129*, No. 104446.
- (35) Lamb, L. E.; Bartolone, S. N.; Ward, E.; Chancellor, M. B. Rapid detection of novel coronavirus/Severe Acute Respiratory Syndrome Coronavirus 2 (SARS-CoV-2) by reverse transcription-loop-mediated isothermal amplification. *PLoS One* **2020**, DOI: [10.1371/journal.pone.0234682](https://doi.org/10.1371/journal.pone.0234682).
- (36) Lu, R.; Wu, X.; Wan, Z.; Li, Y.; Zuo, L.; Qin, J.; Jin, X.; Zhang, C. Development of a novel reverse transcription loop-mediated isothermal amplification method for rapid detection of SARS-CoV-2. *Virol. Sin.* **2020**, *35*, 344–347.
- (37) Park, G.-S.; Ku, K.; Baek, S.-H.; Kim, S.-J.; Kim, S. I.; Kim, B.-T.; Maeng, J.-S. Development of reverse transcription loop-mediated isothermal amplification assays targeting severe acute respiratory syndrome coronavirus 2 (SARS-CoV-2). *J. Mol. Diagn.* **2020**, *22*, 729–735.
- (38) Yan, C.; Cui, J.; Huang, L.; Du, B.; Chen, L.; Xue, G.; Li, S.; Zhang, W.; Zhao, L.; Sun, Y.; et al. Rapid and visual detection of 2019 novel coronavirus (SARS-CoV-2) by a reverse transcription loop-mediated isothermal amplification assay. *Clin. Microbiol. Infect.* **2020**, *26*, 773–779.
- (39) Yu, L.; Wu, S.; Hao, X.; Dong, X.; Mao, L.; Pelechano, V.; Chen, W.-H.; Yin, X. Rapid detection of COVID-19 coronavirus using a reverse transcriptional loop-mediated isothermal amplification (RT-LAMP) diagnostic platform. *Clin. Chem.* **2020**, *66*, 975–977.
- (40) Zhu, X.; Wang, X.; Han, L.; Chen, T.; Wang, L.; Li, H.; Li, S.; He, L.; Fu, X.; Chen, S.; et al. Multiplex reverse transcription loop-mediated isothermal amplification combined with nanoparticle-based lateral flow biosensor for the diagnosis of COVID-19. *Biosens. Bioelectron.* **2020**, *166*, No. 112437.
- (41) Tang, Z.; Nouri, R.; Dong, M.; Yang, J.; Greene, W.; Zhu, Y.; Yon, M.; Nair, M. S.; Kuchipudi, S. V.; Guan, W. Rapid detection of novel coronavirus SARS-CoV-2 by RT-LAMP coupled solid-state nanopores. *Biosens. Bioelectron.* **2022**, *197*, No. 113759.
- (42) Liu, T.; Choi, G.; Tang, Z.; Kshirsagar, A.; Politza, A. J.; Guan, W. Fingerprint Blood-Based Nucleic Acid Testing on A USB Interfaced Device towards HIV self-testing. *Biosens. Bioelectron.* **2022**, *209*, No. 114255.
- (43) Choi, G.; Prince, T.; Miao, J.; Cui, L.; Guan, W. Sample-to-answer palm-sized nucleic acid testing device towards low-cost malaria mass screening. *Biosens. Bioelectron.* **2018**, *115*, 83–90.
- (44) Holstein, C. A.; Griffin, M.; Hong, J.; Sampson, P. D. Statistical method for determining and comparing limits of detection of bioassays. *Anal. Chem.* **2015**, *87*, 9795–9801.